JCTC Journal of Chemical Theory and Computation

PERSPECTIVE

pubs.acs.org/JCTC

Generalized Hartree−Fock Description of Molecular Dissociation

Carlos A. Jiménez-Hoyos,[†] Thomas M. Henderson,[†,‡] and Gustavo E. Scuseria[*,†,‡]

[†]Department of Chemistry, Rice University, 6100 Main Street, Houston, Texas 77005, United States

[‡]Department of Physics and Astronomy, Rice University, 6100 Main Street, Houston, Texas 77005, United States

ABSTRACT: An electronic structure method is said to be size-consistent if the energy of noninteracting fragments is the same when the fragments are treated in a supermolecule approach or are treated in isolation. Size consistency is often violated by Hartree−Fock when symmetries of the exact wave function are imposed on the Hartree−Fock determinant. Relaxing the requirement that the Hartree−Fock wave function be a spin eigenfunction leads to unrestricted Hartree−Fock, which is often (but not always) size-consistent. In this Perspective, we discuss the usually forgotten fact that imposing none of the exact symmetries in what is known as generalized Hartree−Fock allows Hartree−Fock to always be size-consistent and allows size extensive correlated methods such as coupled cluster theory to also be size-consistent. Furthermore, with all symmetries broken, dissociation curves connect the molecule to the fragments better than with symmetries imposed, although the curves are not smooth and show derivative discontinuities akin to unphysical phase transitions. In many cases, correlated dissociation curves based on this generalized Hartree−Fock reference are discontinuous.

1. INTRODUCTION

The past three decades have not been kind to the variational principle in quantum chemistry. Typical state-of-the-art correlated calculations employ some variant of coupled cluster theory,[1−4] which has many strengths but which in practice requires us to abandon the variational principle altogether. Typical mean-field calculations, on the other hand, use some form of Kohn−Sham density functional theory with an approximate exchange-correlation functional; though the variational principle does not hold for these functionals, we blithely apply it nonetheless. Meanwhile, such genuinely variational methods as Hartree−Fock (HF) and configuration interaction have all but disappeared from the computational toolkit, at least in practice.

On the other hand, it should not be forgotten that even in the case of Hartree−Fock, we have not historically taken the variational principle too seriously. That is, we have chosen to constrain the variation in Hartree−Fock by requiring the Hartree−Fock determinant to display at least some of the symmetries of the exact wave function, thereby abandoning full variational flexibility in favor of obtaining more qualitatively correct wave functions. Thus, the restricted Hartree−Fock (RHF) wave function is chosen to be an eigenfunction of the spin operators $\hat{S}^2$ and $\hat{S}_3$, as well as the time-reversal operator $\hat{\Theta}$ and generally the point-group operators $\hat{P}$. The wave function is also usually taken to be real (that is, it is an eigenfunction of the complex conjugation operator $\hat{K}$). The price we pay for preserving these symmetries is that RHF cannot dissociate a closed-shell molecule to the correct open-shell fragments. By this, we mean that RHF is not generally size-consistent, i.e., the energy of a dissociated molecule is not generally equal to the sum of the energies of the dissociation fragments. In unrestricted Hartree−Fock (UHF), we allow the wave function to break symmetry under $\hat{S}^2$ and $\hat{P}$ but not under $\hat{S}_3$ (in other words, we allow for spin contamination and spatial symmetry breaking, but we fix the number of spin-up and spin-down electrons). In simple cases, UHF is size-consistent, but it is not a panacea. The UHF dissociation limits for O_2 and CO_2, for example, are not size-consistent. Generally, UHF correctly dissociates a molecule to UHF fragments only if the open-shell electrons on a given fragment all have the same spin. Occasionally, we must allow the wave function to be complex, i.e., for the density matrix and the orbital coefficients to be complex, although the basis functions may remain real.

Our concern here is with generalized Hartree−Fock (GHF), in which we take the variational principle at face value and impose *none* of the correct symmetries on the Hartree−Fock wave function. The purpose of this paper is to remind the community that if we are willing to sacrifice all symmetries of the wave function by using GHF, then we can dissociate *any* molecule to GHF fragments. The GHF wave function of the dissociated molecule is just the product of the GHF wave functions of the fragments, and the dissociation curve is size-consistent. Generalized Hartree−Fock has seen only limited use, presumably because the wave functions it delivers can be qualitatively unreasonable and good quantum numbers are difficult to recover once lost. On the other hand, achieving size consistency while preserving the symmetries of the wave function is a difficult task.[5−8] Thus, there is a trade off as to what else one wants to do with these wave functions, and for many properties, it is better to keep some symmetries. For molecular dissociations, GHF allows us, in essence, to connect one UHF potential energy curve with another, thus obtaining an energetically reasonable zeroth-order dissociation curve for all bond lengths. The qualitative deficiencies in the GHF wave function can then in principle be corrected by the application of post-GHF correlated methods such as coupled cluster theory, though such corrections are not, as we shall see, without their own problems.

Received: May 21, 2011
Published: July 14, 2011

Table 1. Classification of Hartree−Fock Solutions According to the Symmetries of the Electronic Hamiltonian They Preserve[a]

Fukutome designation	Stuber−Paldus designation	symmetries preserved	structure of orbital coefficient matrix **C**
TICS[b]	real RHF	$\hat{S}^2, \hat{S}_3 \hat{K}, \hat{\Theta}$	$\begin{pmatrix} C_{\sigma\sigma} & 0 \\ 0 & C_{\sigma\sigma} \end{pmatrix}, C \in \mathbb{R}$
CCW[c]	complex RHF	$\hat{S}^2, \hat{S}_3$	$\begin{pmatrix} C_{\sigma\sigma} & 0 \\ 0 & C_{\sigma\sigma} \end{pmatrix}$
ASCW[d]	paired UHF	$\hat{S}_3 \hat{\Theta}$	$\begin{pmatrix} C_{\sigma\sigma} & 0 \\ 0 & C^*_{\sigma\sigma} \end{pmatrix}$
ASDW[e]	real UHF	$\hat{S}_3 \hat{K}$	$\begin{pmatrix} C_{\sigma\sigma} & 0 \\ 0 & C_{\sigma'\sigma'} \end{pmatrix}, C \in \mathbb{R}$
ASW[f]	complex UHF	$\hat{S}_3$	$\begin{pmatrix} C_{\sigma\sigma} & 0 \\ 0 & C_{\sigma'\sigma'} \end{pmatrix}$
TSCW[g]	paired GHF	$\hat{\Theta}$	$\begin{pmatrix} C_{\sigma\sigma} & C_{\sigma\sigma'} \\ -C^*_{\sigma\sigma'} & C^*_{\sigma\sigma} \end{pmatrix}$
TSDW[h]	real GHF	$\hat{K}$	$\begin{pmatrix} C_{\sigma\sigma} & C_{\sigma\sigma'} \\ C_{\sigma'\sigma} & C_{\sigma'\sigma'} \end{pmatrix}, C \in \mathbb{R}$
TSW[i]	complex GHF		$\begin{pmatrix} C_{\sigma\sigma} & C_{\sigma\sigma'} \\ C_{\sigma'\sigma} & C_{\sigma'\sigma'} \end{pmatrix}$

[a] We include the acronyms suggested by both Fukutome[10] and Stuber and Paldus[14] in each of these solutions. The structure of the matrix of orbital coefficients is also included for clarity along with any constraints in the matrix elements. [b] Time-reversal invariant closed-shell. [c] Charge current wave. [d] Axial spin current wave. [e] Axial spin density wave. [f] Axial spin wave. [g] Torsional spin current wave. [h] Torsional spin density wave. [i] Torsional spin wave.

2. GENERALIZED HARTREE−FOCK AND SYMMETRY

Elementary considerations make it clear that if a Hermitian operator $\hat{\Lambda}$ commutes with the Hamiltonian $\hat{H}$, then eigenstates $|\Psi\rangle$ of the Hamiltonian are also eigenstates of $\hat{\Lambda}$ (or can be chosen as such in the case of degeneracies). That is, we have

$$\hat{H}|\Psi\rangle = E|\Psi\rangle \tag{1a}$$

$$\hat{\Lambda}|\Psi\rangle = \lambda|\Psi\rangle \tag{1b}$$

where λ is the eigenvalue of $\hat{\Lambda}$ and is a good quantum number. In the case of the hydrogenic Hamiltonian, for example, the orbital angular momentum operators $\hat{L}^2$ and $\hat{L}_3$ commute with the Hamiltonian, as does the spin operator $\hat{S}_3$. [We have used $\hat{L}_3$ and $\hat{S}_3$ and not $\hat{L}_z$ and $\hat{S}_z$ essentially to indicate that the spatial direction of angular momentum quantization is irrelevant.] Thus, in addition to the principle quantum number n, which labels the energy, we obtain the familiar additional quantum numbers l, m_l, and m_s.

Approximate wave functions need not have all the symmetries of the real wave function (or, in other words, need not have the same good quantum numbers). Forcing an approximate wave function $|\Phi\rangle$ to be symmetry-adapted introduces constraints which reduce variational flexibility. One is forced to choose between finding the variationally optimal wave function and one which has the right symmetries. Löwdin was the first to point out this conundrum, which he called the symmetry dilemma.[9]

A common situation in which one faces the symmetry dilemma is in the dissociation of closed-shell molecules to open-shell fragments. If the Hartree−Fock wave function is optimized by preserving spatial and spin symmetry, then the predicted potential energy curve does not dissociate to the correct limit. On the other hand, allowing the Hartree−Fock wave function to break spatial and spin symmetry enables it to dissociate to the energetically correct limit with, however, a qualitatively incorrect wave function. When we can lower the energy by breaking a symmetry in the Hartree−Fock wave function, we say that the Hartree−Fock wave function is unstable with respect to that symmetry.

It is useful to classify the different solutions according to the self-consistent symmetries they preserve, an effort first undertaken by Fukutome.[10] To make this classification transparent, we must first discuss the symmetries of the electronic Hamiltonian. We note that if there is any symmetry present in the initial guess of the density matrix, then this symmetry will be preserved throughout the optimization procedure. That is, symmetries are self-consistent in the Hartree−Fock equations.

For any molecular system, the wave function $|\Psi\rangle$ must be an eigenfunction of the particle number operator $\hat{N}$. Solutions that break particle number symmetry are rare in quantum chemistry, but it is violated by the Bardeen−Cooper−Schrieffer (BCS) wave function.[11] For net repulsive interactions such as the Coulombic $1/r_{12}$ repulsion between electrons in quantum chemistry, the BCS wave function does not yield an energy lower than the HF wave function.[12] The standard electronic Hamiltonian is additionally invariant to spin rotations and time reversal. Finally, the point-group symmety determined by the nuclear framework is also preserved in exact solutions to the electronic Schrödinger equation.

The fact that the Hamiltonian is invariant to spin rotations implies that the exact eigenfunctions of the electronic Hamiltonian can always be labeled by the s and m_s quantum numbers, corresponding to the spin operators $\hat{S}^2$ and $\hat{S}_3$. The time reversal operator $\hat{\Theta}$ and the complex conjugation operator $\hat{K}$ also commute with the Hamiltonian, but the fact that they are antiunitary operators precludes their association with good quantum numbers.[13]

We will not discuss the group theoretical classification presented by Fukutome in great detail, but Table 1 does show the different Hartree−Fock solutions discussed by Fukutome, as well as the symmetries they preserve. We also include the designation recently suggested by Stuber and Paldus[14] in connection with each of Fukutome's solutions. We emphasize that the solutions we present are independent of the point group symmetry of the molecule; point group symmetry can be separately imposed on the Hartree−Fock wave function or not. Additionally, the classification is valid both for closed-shell and for open-shell wave functions.

Typically, we consider only the real RHF (or ROHF) and real UHF solutions. Complex solutions are known but are rarely sought.[15] While GHF solutions have been explored by Löwdin[16] and others, they are searched for more rarely still, even though Overhauser showed that in the uniform electron gas, the paramagnetic (RHF) state is always unstable with respect to the formation of helical spin density waves (which are GHF states).[17] In quantum chemistry, GHF solutions have been found, for example, in the beryllium atom in some basis sets, in BH, in H_4, and in a few other cases.[10,14,16]

3. HARTREE−FOCK STABILITY

The essence of Hartree−Fock is to find the single determinant which minimizes the expectation value of the Hamiltonian.

In practice, we solve

$$\frac{\partial}{\partial\langle\Phi|}\langle\Phi|\hat{H}|\Phi\rangle = 0 \tag{2}$$

subject to $|\Phi\rangle$ being a normalized determinant. This, of course, guarantees no more than that the energy is stationary. To determine whether or not the energy is a local minimum, we must check the second derivative as well.[18−20]

Determinants can be parametrized in terms of orbital rotations which mix occupied and virtual orbitals. The stationarity condition on the energy is simply

$$\langle\phi_a|\hat{\mathscr{F}}|\phi_i\rangle = 0 \tag{3}$$

where $\hat{\mathscr{F}}$ is the Fock operator and where, here and in the following, indices i and j will refer to occupied orbitals and a and b will refer to virtual orbitals. To check the second derivative of the Hartree−Fock energy, it suffices to check the eigenvalues of the Hartree−Fock orbital Hessian

$$\mathbf{H} = \begin{pmatrix} \mathbf{A} & \mathbf{B} \\ \mathbf{B}^* & \mathbf{A}^* \end{pmatrix} \tag{4}$$

where

$$A_{ia,jb} = \langle\phi_i\phi_b||\phi_a\phi_j\rangle + \langle\phi_b|\hat{\mathscr{F}}|\phi_a\rangle\delta_{ij} - \langle\phi_i|\hat{\mathscr{F}}|\phi_j\rangle\delta_{ab} \tag{5a}$$

$$B_{ia,jb} = \langle\phi_i\phi_j||\phi_a\phi_b\rangle \tag{5b}$$

in terms of the usual antisymmetrized two-electron integrals in Dirac notation. One can restrict the sectors of the Hessian one includes so as to test only for certain types of instabilities. For example, spin-adapting the Hessian searches only for so-called RHF instabilities (instabilities to states which are eigenfunctions of $\hat{S}^2$) and removing spin-flip blocks which mix spin-up occupied orbitals with spin-down virtual orbitals (and vice versa) tests only for RHF and UHF instabilities.

When the orbital Hessian has a negative eigenvalue, a lower energy Hartree−Fock solution exists, which typically displays lower symmetries. The eigenvector associated with this negative eigenvalue distorts the wave function in the direction of the broken symmetry solution. Having followed this eigenvector and obtained the self-consistent broken symmetry solution, we can repeat the stability analysis. At some point, we will converge to a Hartree−Fock solution which is at least locally stable within the manifold under consideration (i.e., has no negative eigenvalues). This solution will generally be one of several degenerate solutions which have broken the same symmetries in different ways. A fact usually unknown in quantum chemistry is that the Hessian corresponding to the broken symmetry solution will have zero eigenvalues, with eigenvectors pointing toward these degenerate solutions, usually known as Goldstone modes. By forming appropriate linear combinations of these broken symmetry solutions, one can restore the symmetry, though not at the single-determinant level.[21,22]

As pointed out by Piecuch et al., when the symmetry broken UHF state is spin projected, the projected wave function contains information about higher level excitations.[23] Presumably, the same is true in the case of projected GHF.

Closely related to the Hartree−Fock orbital Hessian is the random phase approximation (RPA), where one diagonalizes

$$\mathbf{R} = \begin{pmatrix} \mathbf{A} & \mathbf{B} \\ -\mathbf{B}^* & -\mathbf{A}^* \end{pmatrix} \tag{6}$$

to obtain excitation energies of the system. When the Hartree−Fock solution is unstable, the RPA will yield some complex eigenvalues. From the stable but broken symmetry Hartree−Fock state, the RPA matrix will contain zero eigenvalues associated with so-called collective motions that restore the broken symmetry, as already mentioned above.[21]

The much thornier question of whether one has obtained not a local minimum but a global minimum cannot generally be answered in a practical way.

4. MOLECULAR DISSOCIATION

Consider a molecule AB dissociating to well-separated fragments A and B. We will assume that in isolation, fragment A has a GHF wave function $|\Phi_A\rangle$ with energy E_A, and fragment B has a GHF wave function $|\Phi_B\rangle$ and corresponding energy E_B. For the well-separated AB system, we construct the wave function $|\Phi_{AB}\rangle = |\Phi_A\Phi_B\rangle$, which is still of the GHF form. It is not difficult to show (see the Appendix for details) that the energy corresponding to $|\Phi_{AB}\rangle$ is

$$E_{AB} = E_A + E_B + \frac{q_A q_B}{R_{AB}} \tag{7}$$

when the fragments are sufficiently far apart; here, q_A and q_B are the total charges on the two fragments and R_{AB} is the distance between the center of charges of the two fragments. Clearly, in the limit of infinite separation, our wave function $|\Phi_{AB}\rangle$ yields the correct dissociation limit, $E_{AB} = E_A + E_B$. In other words, nothing prevents the most general Hartree−Fock wave function from correctly dissociating to generalized Hartree−Fock fragments. Dissociation to multiple fragments is also shown to be correct by the foregoing, essentially in a recursive manner (i.e., $E_{ABC} = E_{AB} + E_C = E_A + E_B + E_C$).

That this result does not hold in general for RHF or UHF wave functions is well-known, and the reason for this failure is quite simple: the UHF and particularly the RHF wave functions enforce symmetries which exclude $|\Phi_{AB}\rangle$ from the variational space. In the case of H_2 at infinite separation, for example, $|\Phi_{AB}\rangle$ cannot be an RHF wave function because $|\Phi_{AB}\rangle = |\Phi_A\Phi_B\rangle$ is not an eigenfunction of $\hat{S}^2$. In the case of O_2 at infinite separation, as we shall see, UHF can only obtain the correct dissociation limit with $m_S = 0$ or $m_S = \pm 2$; neither of these connect to the UHF ground state wave function at equilibrium, which has $m_S = \pm 1$. The GHF wave function, however, simply reduces to the UHF triplet near equilbrium ($m_S = \pm 1$) and at dissociation to the UHF singlet ($m_S = 0$), because it does not conserve m_S.

5. RESULTS

The RHF, UHF, and GHF calculations shown in this work have been performed using a development version of the *Gaussian* suite of programs.[24,25] We have carried out correlated calculations at second order in perturbation theory (MP2), as well as with coupled cluster doubles[1,2] (CCD) and coupled cluster singles and doubles[26−30] (CCSD). Correlated calculations on

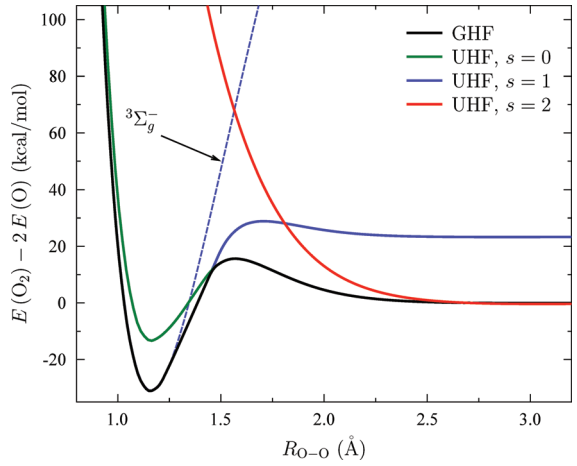

Figure 1. Dissociation curves of the oxygen molecule computed at the HF level. The zero of energy has been set at the energy of two triplet UHF oxygen atoms. We show the lowest energy UHF singlet, triplet, and quintet solutions, as well as the symmetric UHF triplet. The GHF curve connects the UHF triplet solution at equilibrium with the UHF singlet solution for $r \gtrsim 1.5$ Å.

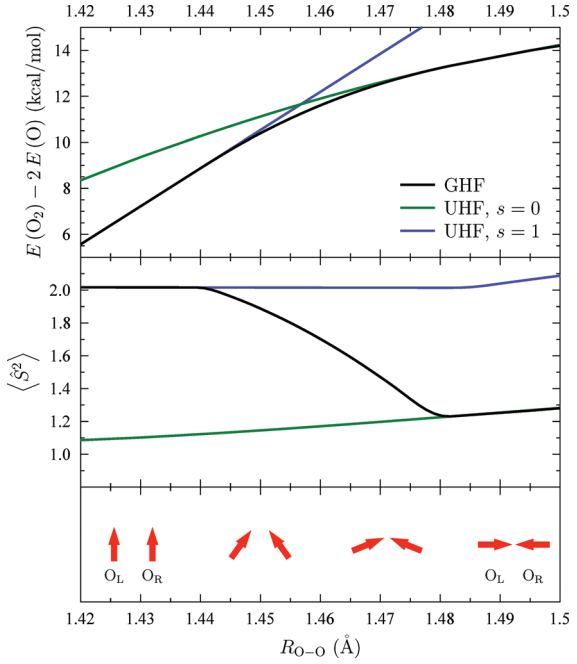

Figure 2. Top panel: Zoom-in of the region of the dissociation curve of O_2 where a GHF solution is lower than either of the UHF solutions. Middle panel: Expectation value of $\hat{S}^2$ for the broken symmetry UHF singlet, UHF triplet, and GHF solutions. Note that $\langle \hat{S}^2 \rangle$ diminishes for the GHF solution when it goes from the triplet UHF solution and merges into the spin-contaminated singlet solution. Bottom panel: Mulliken atomic densities of the two oxygen atoms (left and right) as a function of the bond length for the GHF solution. Observe how the spin densities rotate from being parallel for $r < 1.42$ Å to being antiparallel for $r > 1.5$ Å.

RHF and UHF references were done using *Gaussian*, while those calculations on GHF references were done using an in-house program which reads the GHF eigenvectors from *Gaussian* and which works in the spinorbital basis. We verified the correctness of this program by comparison to *Gaussian*'s MP2, CCD, and CCSD results for RHF and UHF references, as well as for rotated UHF references (i.e., UHF references in which the wave function is an eigenfunction of $\hat{S}_x$ rather than of $\hat{S}_z$).

All GHF solutions reported in this work are real GHF solutions, and we did not find any complex solutions with lower energy than the GHF solutions shown. *Gaussian* does not have the capability of analyzing the stability of GHF-type wave functions, though there is the capability to test whether UHF solutions are GHF-stable. Thus, we cannot guarantee that there are no GHF solutions other than those we are reporting. We did generate a variety of different initial guesses in an attempt to recover as many GHF solutions as possible. In selected cases, we have tested the stability of GHF solutions using our in-house program.

Throughout, we have used Dunning's cc-pvdz basis set[31] with Cartesian *d* functions. While this basis is of minimal utility for high-accuracy prediction of molecular properties using correlated wave functions, it should be adequate for our purpose, which is simply to show the qualitative features of GHF and post-GHF calculations.

5.1. Dissociation of O_2. Let us begin by considering O_2. In the ground state, O_2 dissociates through the $^3\Sigma_g^-$ surface into two ^3P oxygen atoms. Describing triplet O_2 at the UHF level requires us to have $m_S = \pm 1$, while describing two triplet oxygen atoms with UHF requires each atom to have $m_S = \pm 1$ and the overall system to therefore have $m_S = 0$ or $m_S = \pm 2$.

There are, then, three relevant broken symmetry UHF states for our purposes, shown in Figure 1 along with the symmetry preserving UHF solution $^3\Sigma_g^-$. The triplet UHF curve at equilibrium cannot properly dissociate into two triplet atoms. Both the broken-symmetry singlet ($m_S = 0$) and quintet ($m_S = \pm 2$) curves are excited states at equilibrium but correctly dissociate to two triplet atoms, which the singlet approaches from below and the quintet approaches from above. It is clear that the triplet curve must cross both the singlet and the quintet. What we might prefer is to follow the UHF triplet solution near equilibrium and the UHF singlet near dissociation. This is precisely what GHF delivers: the lowest energy GHF solution connects the broken symmetry UHF triplet solution at equilibrium with the broken symmetry UHF singlet solution for $r \gtrsim 1.5$ Å. In this case, the GHF dissociation curve is differentiable but not smooth. At dissociation, the orbitals are localized onto the atoms and become the GHF atomic orbitals, exactly as we would expect for a product wave function of the form $|\Phi_{AB}\rangle = |\Phi_A \Phi_B\rangle$.

Figure 2 zooms in on the region where the UHF triplet and singlet cross. There is a small region over which a GHF solution exists, connecting the two surfaces. In Figure 2, we show how the GHF solution rotates the spin densities on the oxygen atoms from being parallel for $r < 1.42$ Å to being antiparallel for $r > 1.5$ Å, where the GHF solution coincides with the broken symmetry singlet solution. The expectation value of $\hat{S}^2$ goes down until it merges with the curve corresponding to the spin-contaminated singlet solution.

In Figure 3, we show the coupled-cluster results for the dissociation of O_2 on the singlet and triplet UHF references and on the GHF reference, as well as the corresponding reference dissociation curves. Using the UHF triplet as a reference, coupled cluster is not size-consistent, but using the GHF curve as a reference, it is. In the case of CCD (as well as MP2, not shown) the curves are continuous using a GHF reference. However, the CCSD curve on the GHF reference appears to be discontinuous.

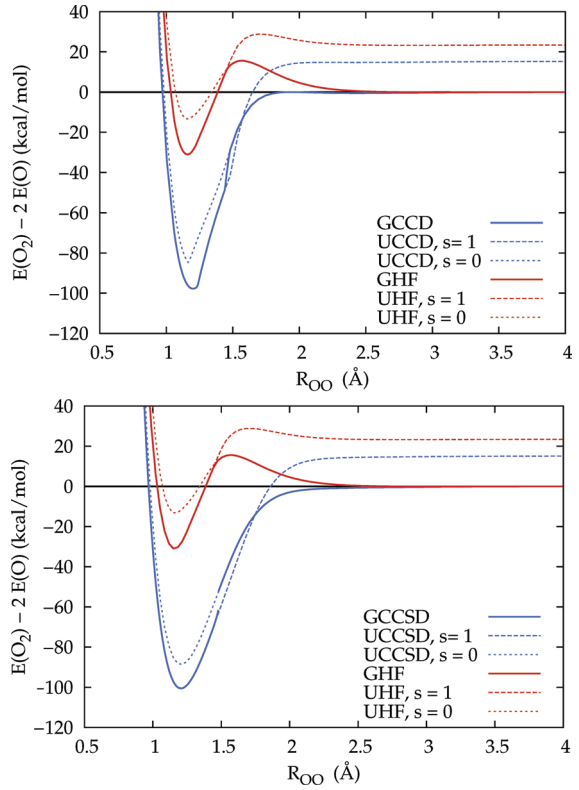

Figure 3. Top Panel: Coupled-cluster doubles and Hartree−Fock curves for the dissociation of O_2. Bottom Panel: Coupled-cluster singles and doubles and Hartree−Fock curves for the dissociation of O_2. The zero of energy has been set at the energy of two triplet oxygen atoms.

This can be readily understood in the following way: The effect of single excitations is simply to rotate the orbitals.[18] In the region of the potential energy curve where GHF is distinct from the UHF triplet, the single excitations will thus rotate the GHF reference toward the UHF triplet reference (and indeed, we see very little difference in their energy). Where the GHF joins the UHF singlet, however, the standard initial guess for the single excitation amplitudes forces CCSD to preserve $m_S = 0$. Since the CCSD curves based on the UHF singlet and triplet do not intersect at the same point as do the reference Hartree−Fock curves, we therefore see a discontinuity in the CCSD curve. The discontinuities in the CCSD curve appear to be, in other words, essentially due to abrupt changes in the character of the reference determinant and not due to the existence of multiple solutions to the CCSD equations *per se*. It may be that with a sufficiently clever initial guess that rotates the UHF singlet toward the UHF triplet, the CCSD curve can be made continuous, though we cannot guarantee this. The results of Li and Paldus[32] suggest that configuration interaction based on the GHF curve would quite probably be smoother, though no longer size-consistent. Because we use the lowest energy UHF solution as a reference at every geometry, the CCD and MP2 curves behave somewhat erratically where the UHF solution bifurcates.

If we were to continue to increase the level of correlation, the coupled-cluster curve based on the UHF triplet would improve, particularly near dissociation. Presumably the coupled-cluster curve based on the GHF reference would do likewise, provided with the correct initial guess. In Figure 4, we show the CCSD(T)[33] curves using the singlet and triplet UHF references.

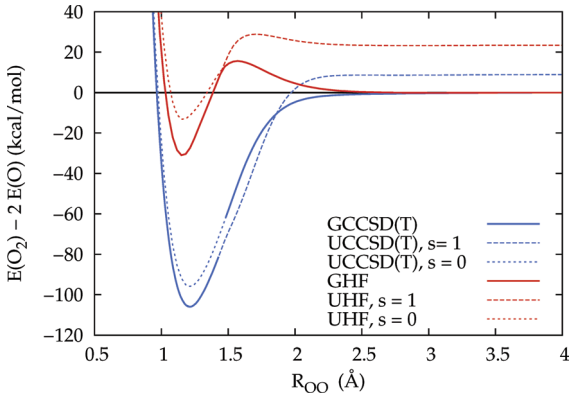

Figure 4. Hartree−Fock and CCSD(T) curves for the dissociation of O_2. The zero of energy has been set at the energy of two triplet oxygen atoms. Comparison with Figure 3 shows that CCSD(T) and CCSD have no qualitative differences in this case. The curve marked as the GHF-based CCSD(T) uses the UHF triplet as a reference for small R and the UHF singlet as a reference for large R.

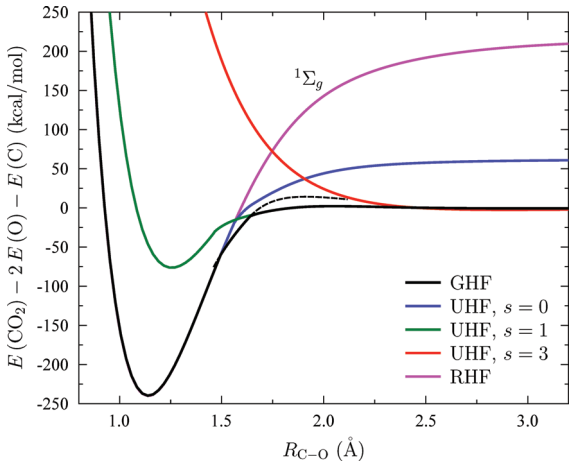

Figure 5. Dissociation curves of the CO_2 molecule into a carbon atom and a pair of oxygen atoms, computed at the HF level. The zero of energy has been set at the energy of UHF triplet atoms. We show the lowest energy UHF singlet, triplet, and septet solutions as well as the RHF solution and two GHF solutions. There are two kinks in the lowest energy GHF curve, as can be seen more clearly in Figure 6.

The curve marked as using the GHF reference in fact uses one of the two UHF states as a reference in the region where the GHF and UHF states are identical. We have not included data from the region where GHF is distinct from UHF, as we do not have a genuine GHF-based CCSD(T) implementation. Qualitatively, there is little distinction between the CCSD and CCSD(T) results, which is to be expected, though we note that indeed the difference between the singlet and triplet dissociation limits for CCSD(T) is less than the corresponding difference for CCD or CCSD. Eventually, as we reach full configuration interaction, the UHF-based and GHF-based coupled cluster curves would coincide. Finally, we point out that while GHF does go to the right limit, it does so with an artificial barrier to the formation of the bond in O_2. This is much in analogy with the behavior of UHF in N_2, which likewise goes to the proper limit but with an unphysical bump. Adding explicit correlations, as expected, eliminates the bump.

dx.doi.org/10.1021/ct200345a |J. Chem. Theory Comput. 2011, 7, 2667–2674

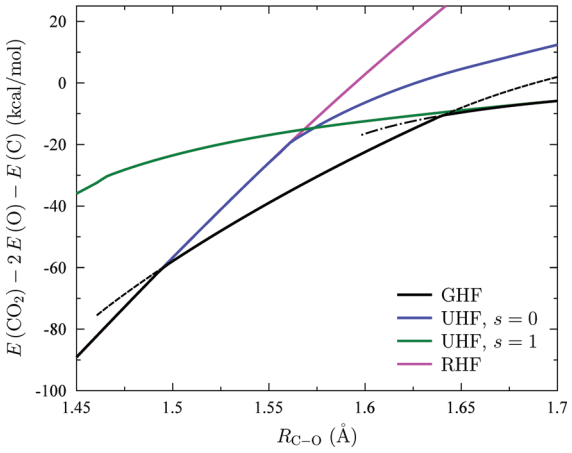

Figure 6. Zoom-in of the region of the symmetric dissociation curve of CO_2 where GHF solutions are lower than any of the UHF solutions. Three different GHF solutions were found in the interval 1.4 Å < r < 1.7 Å. None of the solutions connect smoothly with the RHF/UHF curve. We have succeeded in following the GHF solutions a short way past the point where they cross various UHF solutions.

5.2. Symmetric Dissociation of CO_2. Now, we turn to the description of the atomization of CO_2 by symmetric stretching of the C═O bonds. The ground state dissociation occurs through the $^1\Sigma_g$ surface into two ^3P oxygen atoms and a ^3P carbon atom. At the UHF level, the appropriate dissociation limit can then only be reached with $m_S = \pm 3$ and $m_S = \pm 1$, though at equilibrium the system must clearly have $m_S = 0$.

Dissociation curves computed at the HF level are shown in Figure 5. This figure includes the symmetric RHF solution $^1\Sigma_g$, which has a triplet instability for r > 1.6 Å, yielding the singlet UHF solution. Several broken symmetry triplet solutions were found, the lowest energy of which is included in the figure, as is the broken symmetry septet solution. The lowest energy GHF solution has two kinks, as explained below.

In Figure 6, we zoom in on the region of the potential energy curve where the various UHF solutions cross each other. Three different GHF solutions were found. The first (dashed in Figure 6) crosses the RHF solution near r = 1.5 Å; we can continue to follow this solution to $r \approx$ 1.46 Å, but no further. This same GHF solution crosses the UHF triplet near r = 1.64 Å and can be followed until $r \approx$ 2.1 Å. The second GHF solution (dashed-dotted in Figure 6) connects to the UHF broken-symmetry triplet and crosses the first GHF solution near r = 1.64 Å. A third solution can also be found in this vicinity, but it is slightly higher in energy.

While we can continuously follow various GHF curves from the RHF solution at equilibrium to the UHF triplet at dissociation, the result is not differentiable due to the kinks mentioned above. We looked for other GHF solutions near these kinks, to smooth the transition from one curve to another, but were unable to find any. Stability analyses every 0.005 Å between 1.5 Å and 1.65 Å revealed no GHF instabilities in our solutions. We have used a quadratically convergent algorithm[34] to follow solutions as far as possible.

In Figure 7, we show the results from MP2 based on the GHF reference. While the MP2 curve on the GHF reference is continuous in O_2, it is discontinuous here. This is simply because, unlike in O_2 where the GHF solution merges with the UHF triplet and UHF singlet, here in CO_2 the GHF solutions, as we

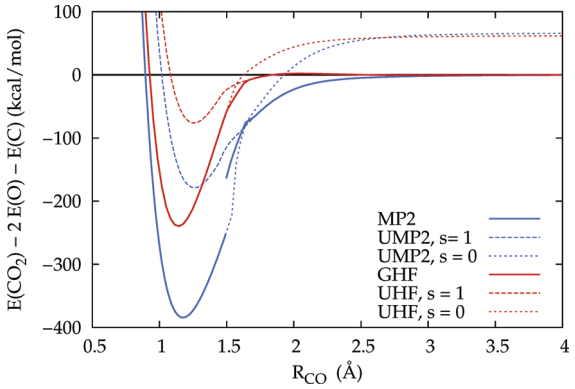

Figure 7. Second-order and Hartree−Fock curves for the dissociation of CO_2. The zero of energy has been set at the energy of isolated atoms. The GHF-based MP2 curve connects the two UHF-based curves, with a jump where the GHF and UHF singlet solution merge.

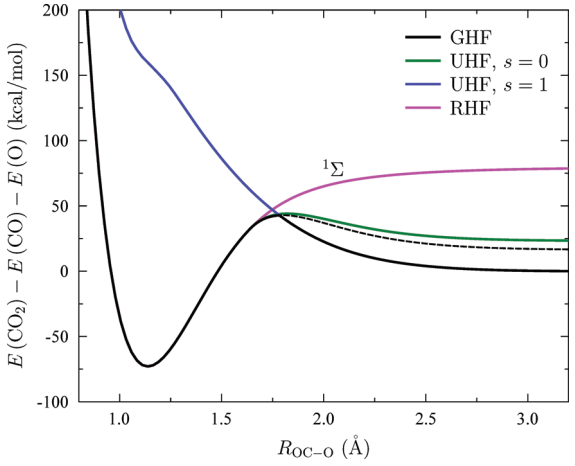

Figure 8. Dissociation curves of CO_2 molecule into an oxygen atom and the CO molecule, computed at the HF level. One of the C−O distances has been kept constant at r = 1.1621 Å. We show the symmetric RHF curve, the broken-symmetry UHF singlet and triplet, and two GHF solutions.

have already noted, continue past the points where they cross the RHF and UHF triplet curves. Thus, unlike in O_2, the orbitals and orbital energies on the lowest-energy Hartree−Fock reference change abruptly at the curve crossings, and the MP2 becomes discontinuous. Coupled cluster will inherit these same deficiencies.

5.3. Asymmetric Dissociation of CO_2. The last example we consider corresponds to the asymmetric dissociation of the CO_2 into an oxygen atom and CO. In the ground state, this process occurs through the $^1\Sigma$ surface dissociating into a ^3P oxygen atom and a $^1\Sigma^+$ CO molecule. Thus, only a triplet solution will yield the right dissociation limit at the Hartree−Fock level.

Dissociation curves computed at the HF level are shown in Figure 8. We show the symmetric RHF solution $^1\Sigma$ along with a broken symmetry singlet UHF solution. Figure 8 also shows the lowest energy triplet UHF solution, which is unbound but which goes to the energetically correct dissociation limit. Finally, we include two GHF solutions. The lowest energy GHF curve shows a kink near r = 1.8 Å, where the triplet and UHF singlet cross. Note that there is another solution which is bound and has lower energy for small interatomic separations.

dx.doi.org/10.1021/ct200345a |J. Chem. Theory Comput. 2011, 7, 2667–2674

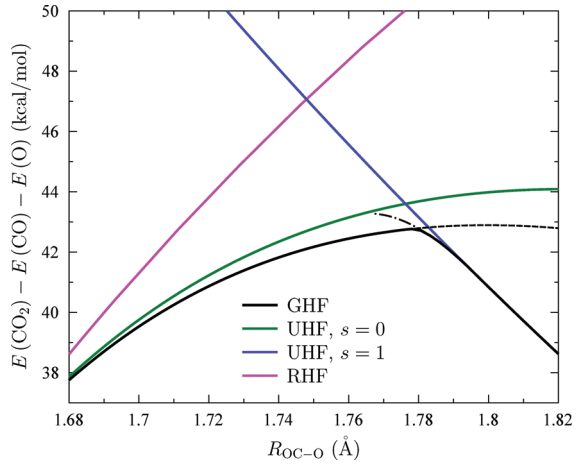

Figure 9. Zoom-in of the region of the asymmetric dissociation curve of CO_2 where GHF solutions are lower than any of the UHF solutions. Note how one of the GHF solutions merges with the singlet UHF solution for $r < 1.65$ Å. On the other hand, another GHF solution merges with the UHF triplet solution for $r > 1.8$ Å. At $r \approx 1.78$ Å, the two GHF solutions intersect.

Figure 9 zooms in on the region of the potential energy surface where GHF connects the singlet and triplet UHF states. Of our two GHF solutions, one connects to the singlet and the other to the triplet. These two solutions intersect at $r \approx 1.78$ Å, and we were unable to find other GHF solutions which connect them smoothly. Stability analysis of the lowest energy GHF solution every 0.005 Å between 1.77 Å and 1.80 Å revealed no GHF instabilities.

6. DISCUSSION

As we have seen, relaxing all of the symmetry constraints allows for Hartree−Fock to reach the energetically correct dissociation limit for several molecules for which RHF and UHF are not size-consistent. The price we pay for having the right behavior at equilibrium and size-consistent dissociation is that the GHF dissociation curve is not always smooth or even always differentiable. This is in analogy with UHF instabilities, where the wave function need not have continuous derivatives, but the situation appears to be somewhat exacerbated in GHF. We point out that due to the nonlinearity of the Hartree−Fock equations, this same phenomenon may exist in following the lowest energy RHF or UHF solution at each geometry. It is also worth noting that often one can find myriad GHF solutions which, however, cannot always be followed from one nuclear configuration to another. In other words, GHF is a rather tricky method. We point the interested reader to work by Fukutome[35] and Mestechkin[36] on the properties of the potential energy surface near a Hartree−Fock instability threshold and to work of Fukutome[37−39] on molecular dissociation.

Post-GHF correlated calculations inherit the same problems as does GHF. Worse, when GHF solutions cross rather than merge with higher symmetry solutions, correlated curves using the GHF reference may be discontinuous. Additionally, the inclusion of single excitations may be problematic, and one presumably needs a fairly clever initial guess to force solutions which carry the wave function from one symmetry to another (for example, changing the value of m_S from 0 to 1 in the dissociation of O_2). Configuration interaction may not inherit these same problems, simply because rather than solving nonlinear equations one merely diagonalizes the Hamiltonian in a restricted space which can be chosen to include spin flips. On the other hand, truncated configuration interaction is not size-extensive, and for all of their qualitative weaknesses, it should not be forgotten that size-extensive correlated techniques such as many-body perturbation theory or coupled cluster theory in combination with a size-consistent reference such as GHF result in size-consistent correlated methods, which is not generally the case when these same techniques are applied to a reference which is not size-consistent.

APPENDIX A. GHF AND SIZE CONSISTENCY

Let us return to our GHF-type wave function for the well-separated AB system, $|\Phi_{AB}\rangle = |\Phi_A\Phi_B\rangle$, where we recall that $|\Phi_A\rangle$ and $|\Phi_B\rangle$ are the GHF wave functions for the isolated fragments A and B, respectively. The total energy of the system, including the nuclear−nuclear repulsion energy, is then

$$\begin{aligned} E_{AB} &= E_{AB}^{nuc} + E_A^{nuc} + E_B^{nuc} + \sum\langle\phi_A|h|\phi_A\rangle \\ &\quad + \sum\langle\phi_B|h|\phi_B\rangle + \frac{1}{2}\sum\langle\phi_A\phi_{A'}||\phi_A\phi_{A'}\rangle \\ &\quad + \frac{1}{2}\sum\langle\phi_B\phi_{B'}||\phi_B\phi_{B'}\rangle + \sum\langle\phi_A\phi_B||\phi_A\phi_B\rangle \end{aligned} \tag{8}$$

where E_A^{nuc}, E_B^{nuc}, and E_{AB}^{nuc} are, respectively, the nuclear repulsion energy within fragment A within fragment B and between fragments A and B, and where ϕ_A and ϕ_B are molecular orbitals occupied in $|\Phi_A\rangle$ and $|\Phi_B\rangle$. $h = t + v_A + v_B$, where v_i represents interactions with the nuclei in fragment i, the total energy becomes simply

$$\begin{aligned} E_{AB} &= E_A + E_B + E_{AB}^{nuc} + \sum\langle\phi_A|v_B|\phi_A\rangle \\ &\quad + \sum\langle\phi_B|v_A|\phi_B\rangle + \sum\langle\phi_A\phi_B||\phi_A\phi_B\rangle \end{aligned} \tag{9}$$

The exchange energy between the two fragments vanishes since the orbitals do not overlap, and the remaining integrals can all be evaluated using the multipole expansion. The result is

$$E_{AB} = E_A + E_B + \frac{(Z_A - N_A)(Z_B - N_B)}{R_{AB}} + \mathcal{O}\left(\frac{1}{R_{AB}^2}\right) \tag{10}$$

where Z_i and N_i are, respectively, the total nuclear charge and the total number of electrons in fragment i. Recognizing $Z_i - N_i = q_i$ gives us eq 7.

AUTHOR INFORMATION

Corresponding Author
*E-mail: guscus@rice.edu.

ACKNOWLEDGMENT

This work was supported by the National Science Foundation (Grants CHE-0807194 and CHE-1110884) and the Welch Foundation (C-0036). We thank Juan Peralta for providing us with the code necessary for population analysis on a GHF wave function.

REFERENCES

(1) Čížek, J. *J. Chem. Phys.* **1966**, *45*, 4256.

(2) Čížek, J. *Adv. Chem. Phys.* **1969**, *14*, 35.
(3) Paldus, J.; Li, X. Z. *Adv. Chem. Phys.* **1999**, *110*, 1.
(4) Shavitt, I.; Bartlett, R. J. *Many-Body Methods in Chemistry and Physics*; Cambridge University Press: New York, 2009.
(5) Tsuchimochi, T.; Scuseria, G. E. *J. Chem. Phys.* **2009**, *131*, 121102.
(6) Scuseria, G. E.; Tsuchimochi, T. *J. Chem. Phys.* **2009**, *131*, 164119.
(7) Tsuchimochi, T.; Scuseria, G. E.; Savin, A. *J. Chem. Phys.* **2010**, *132*, 024111.
(8) Tsuchimochi, T.; Henderson, T. M.; Scuseria, G. E. *J. Chem. Phys.* **2010**, *133*, 134108.
(9) Löwdin, P.-O.; Lykos, P.; Pratt, G. W. *Rev. Mod. Phys.* **1963**, *35*, 496–501.
(10) Fukutome, H. *Int. J. Quantum Chem.* **1981**, *20*, 955–1065.
(11) Bardeen, J.; Cooper, L. N.; Schrieffer, J. R. *Phys. Rev.* **1957**, *108*, 1175–1204.
(12) Bach, V.; Lieb, E. H.; Solovej, J. P. *J. Stat. Phys.* **1994**, *76*, 3.
(13) Wigner, E. P. *J. Math. Phys.* **1960**, *1*, 409.
(14) Stuber, J. L.; Paldus, J. Symmetry Breaking in the Independent Particle Model. In *Fundamental World of Quantum Chemistry: A Tribute Volume to the Memory of Per-Olov Löwdin*; Brändas, E. J., Kryachko, E. S., Eds.; Kluwer Academic Publishers: Dordrecht, The Netherlands, 2003; Vol. 1, Chapter 4, pp 67−139.
(15) Benard, M. *J. Chem. Phys.* **1969**, *71*, 2546–2556.
(16) Löwdin, P.-O.; Mayer, I. *Adv. Quantum Chem.* **1992**, *24*, 79–114.
(17) Overhauser, A. W. *Phys. Rev.* **1962**, *128*, 1437–1452.
(18) Thouless, D. J. *Nucl. Phys.* **1960**, *21*, 225–232.
(19) Čížek, J.; Paldus, J. *J. Chem. Phys.* **1967**, *47*, 3976–3985.
(20) Seeger, R.; Pople, J. A. *J. Chem. Phys.* **1977**, *66*, 3045–3050.
(21) Blaizot, J.-P.; Ripka, G. *Quantum Theory of Finite Systems;* MIT Press: Cambridge, MA, 1985.
(22) Scuseria, G. E.; Jiménez-Hoyos, C. A.; Henderson, T. M.; Samanta, K.; Ellis, J. K. *Projected Quasiparticle Theory for Molecular Electronic Structure*. http://arxiv.org/abs/1106.0956. Submitted for publication.
(23) Piecuch, P.; Toboła, R.; Paldus, J. *Phys. Rev. A* **1996**, *54*, 1210.
(24) Frisch, M. J.; Trucks, G. W.; Schlegel, H. B.; Scuseria, G. E.; Robb, M. A.; Cheeseman, J. R.; Scalmani, G.; Barone, V.; Mennucci, B.; Petersson, G. A.; Nakatsuji, H.; Caricato, M.; Li, X.; Hratchian, H. P.; Izmaylov, A. F.; Bloino, J.; Zheng, G.; Sonnenberg, J. L.; Hada, M.; Ehara, M.; Toyota, K.; Fukuda, R.; Hasegawa, J.; Ishida, M.; Nakajima, T.; Honda, Y.; Kitao, O.; Nakai, H.; Vreven, T.; Montgomery, J. A., Jr.; Peralta, J. E.; Ogliaro, F.; Bearpark, M.; Heyd, J. J.; Brothers, E.; Kudin, K. N.; Staroverov, V. N.; Kobayashi, R.; Normand, J.; Raghavachari, K.; Rendell, A.; Burant, J. C.; Iyengar, S. S.; Tomasi, J.; Cossi, M.; Rega, N.; Millam, J. M.; Klene, M.; Knox, J. E.; Cross, J. B.; Bakken, V.; Adamo, C.; Jaramillo, J.; Gomperts, R.; Stratmann, R. E.; Yazyev, O.; Austin, A. J.; Cammi, R.; Pomelli, C.; Ochterski, J. W.; Martin, R. L.; Morokuma, K.; Zakrzewski, V. G.; Voth, G. A.; Salvador, P.; Dannenberg, J. J.; Dapprich, S.; Parandekar, P. V.; Mayhall, N. J.; Daniels, A. D.; Farkas, O.; Foresman, J. B.; Ortiz, J. V.; Cioslowski, J.; Fox, D. J. *Gaussian Development Version*, Revision H.01; Gaussian, Inc.: Wallingford, CT, 2009.
(25) Peralta, J. E.; Scuseria, G. E.; Frisch, M. J. *Phys. Rev. B* **2007**, *75*, 125119.
(26) Purvis, G. D., III; Bartlett, R. J. *J. Chem. Phys.* **1982**, *76*, 1910.
(27) Cullen, J. M.; Zerner, M. C. *J. Chem. Phys.* **1982**, *77*, 4088–4109.
(28) Scuseria, G. E.; Lee, T. J.; Schaeffer, H. F. *Chem. Phys. Lett.* **1986**, *130*, 236–239.
(29) Scuseria, G. E.; Schaeffer, H. F. *Chem. Phys. Lett.* **1988**, *146*, 23–31.
(30) Piecuch, P.; Paldus, J. *Int. J. Quantum Chem.* **1989**, *36*, 429.
(31) Dunning, T. H., Jr. *J. Chem. Phys.* **1989**, *90*, 1007.
(32) Li, X.; Paldus, J. *J. Chem. Phys.* **2009**, *130*, 084110.
(33) Raghavachari, K.; Trucks, G.; Pople, J. A.; Head-Gordon, M. *Chem. Phys. Lett.* **1989**, *157*, 479.
(34) Bacskay, G. B. *Chem. Phys.* **1981**, *61*, 385–404.
(35) Fukutome, H. *Prog. Theor. Phys.* **1975**, *53*, 1320–1336.
(36) Mestechkin, M. *THEOCHEM* **1988**, *181*, 231–236.
(37) Takabe, T.; Takahashi, M.; Fukutome, H. *Prog. Theor. Phys.* **1976**, *56*, 349.
(38) Takahashi, M.; Fukutome, H. *Prog. Theor. Phys.* **1978**, *59*, 1787.
(39) Igawa, A.; Fukutome, H. *Prog. Theor. Phys.* **1980**, *64*, 491.